EPJ Web of Conferences **274**, 01007 (2022) https://doi.org/10.1051/epjconf/202227401007
XVth Quark Confinement and the Hadron Spectrum

Thermal Axions: What's next?

Francesco D'Eramo[1, 2,*]

[1]Dipartimento di Fisica e Astronomia, Università degli Studi di Padova, Via Marzolo 8, 35131 Padova, Italy
[2]Istituto Nazionale di Fisica Nucleare (INFN), Sezione di Padova, Via Marzolo 8, 35131 Padova, Italy

Abstract. Scattering and decay processes of thermal bath particles in the early universe can dump relativistic axions in the primordial plasma. If produced with a significant abundance, their presence can leave observable signatures in cosmological observables probing both the early and the late universe. We focus on the QCD axion and present recent and significant improvements for the calculation of the axion production rate across the different energy scales during the expansion of the universe. We apply these rates to predict the abundance of produced axions and to derive the latest cosmological bounds on the axion mass and couplings.

1 Introduction

The Peccei-Quinn (PQ) mechanism [1, 2] is an elegant solution to the experimentally observed invariance of strong interactions when we flip the arrow of time. For each microscopic realization, the framework features a global symmetry $U(1)_{\rm PQ}$ that must satisfy two key requirements: spontaneously broken, and anomalous under the color gauge group of the standard model. The scale of spontaneous PQ breaking is bound to be much higher than the energies experimentally accessible, and the only low-energy residual is a pseudo-Nambu-Goldstone boson (PNGB) known as the QCD axion [3, 4]. The color anomaly imposes a coupling of the axion field a to gluons via the dimension 5 operator

$$\mathcal{L}_{\rm PQ} \supset \frac{\alpha_s}{8\pi}\frac{a}{f_a}G^A_{\mu\nu}\widetilde{G}^{A\mu\nu} \,. \tag{1}$$

This operator defines the axion decay constant f_a. We have above the QCD fine structure constant $\alpha_s = g_s^2/(4\pi)$, the gluon field strength tensor $G^a_{\mu\nu}$, and its dual $\widetilde{G}^{a\mu\nu}$. Interactions with other standard model fields are model dependent, and given its PNGB nature all axion couplings are suppressed by the scale f_a. Broadly speaking, there are two classes of axion couplings to visible matter

$$\mathcal{L}_{\rm axion-int} \supset \frac{1}{f_a}\left[a\, c_X \frac{\alpha_X}{8\pi} X^{a\mu\nu}\widetilde{X}^a_{\mu\nu} + \partial_\mu a\; c_\psi \overline{\psi}\gamma^\mu\psi\right] . \tag{2}$$

The first class contains couplings to standard model gauge bosons ($X = \{G, W, B\}$), and we set $c_G = 1$ consistently with Eq. (1). The standard model fermions appearing in the

*e-mail: francesco.deramo@pd.infn.it

second class have defined electroweak quantum numbers ($\psi = \{Q_L, u_R, d_R, L_L, e_R\}$), and their interactions preserve the shift symmetry $a \rightarrow a + \text{const}$. QCD non-perturbative effects generate a potential once strong interactions confine, and this leads to an axion mass [5]

$$m_a \simeq 5.7\,\mu eV \left(\frac{10^{12}\,\text{GeV}}{f_a}\right). \tag{3}$$

Famously, the QCD axion is a viable dark matter candidate [6–8]. We focus on thermal axions in Sec. 2, and we give updated predictions for the KSVZ [9, 10] and DFSZ [11, 12] frameworks. We provide in Sec. 3 cosmological bounds on flavor-violating axion couplings, and in Sec. 4 an updated cosmological bound on the QCD axion mass. We conclude in Sec. 5.

2 Axion Dark Radiation

A contribution to the cold dark matter abundance is far from being the only cosmological feature of PQ theories. The PQ framework leads to other fascinating phenomena in the early universe with testable consequences today. In what follows, we consider axions produced in the early universe with kinetic energy much larger than their rest mass. Several production mechanisms can be responsible for this additional population of hot axions. Regardless of the specific mechanism, their energy gets depleted with the expansion and the overall energy density behaves as radiation as long as these axions remain relativistic. Thus their effect is an additional contribution to the radiation energy density, and we measure this quantity by investigating the formation of light nuclei via Big Bang Nucleosynthesis (BBN) and the formation of the Cosmic Microwave Background (CMB). Historically, this effect has been quantified in terms of a modification of the total number of neutrino species. The effective number of neutrinos N_{eff} is related to the radiation energy density ρ_{rad} as

$$\rho_{\text{rad}} = \rho_\gamma \left[1 + \frac{7}{8}\left(\frac{T_\nu}{T_\gamma}\right)^4 N_{\text{eff}}\right]. \tag{4}$$

Any relativistic particle with a substantial energy density, like the axions, will contribute to N_{eff}. We look for deviations from the standard cosmological value ($N_{\text{eff}}^{\Lambda\text{CDM}} = 3.044$)

$$\Delta N_{\text{eff}} \equiv N_{\text{eff}} - N_{\text{eff}}^{\Lambda\text{CDM}} = \frac{8}{7}\left(\frac{11}{4}\right)^{4/3} \frac{\rho_a}{\rho_\gamma}. \tag{5}$$

We focus here on thermal production channels. The QCD axion couples to gluons via the anomalous dimension 5 interaction given in Eq. (1). Couplings to other standard model particles are model dependent, and they are typically present (perhaps loop-suppressed) unless unnatural cancellations are in action. Thermal production is, in some sense, an unavoidable injection source since it only assumes the existence of a thermal bath at early times. For every specific model, the amount of axions produced thermally is determined unless we move away from a standard cosmological history. The leading production channels are binary scatterings and decays that produce relativistic axions because they are efficient above BBN, and they subsequently red-shift with the expansion until they get to the non-relativistic regime. Such a transition can happen quite late. As a rule of thumb, the axion phase-space distribution stays thermal with a temperature not too much different from the ones of the radiation bath (given their thermal origin). Therefore they manifest themselves as additional radiation at BBN if $m_a \lesssim \text{MeV}$, and at recombination if $m_a \lesssim 0.3\,\text{eV}$.

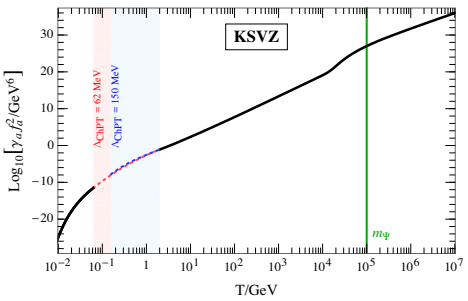

Figure 1. Production rate as a function of the temperature for the KSVZ axion (from Ref. [18]).

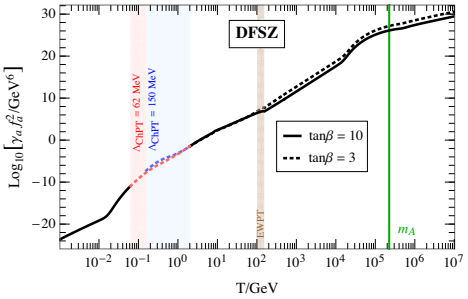

Figure 2. Production rate as a function of the temperature for the DFSZ axion (from Ref. [18]).

We track the hot axion population in the early universe via the Boltzmann equation for the axion number density

$$\frac{dn_a}{dt} + 3Hn_a = \gamma_a \left(1 - \frac{n_a}{n_a^{\rm eq}}\right) . \tag{6}$$

The left hand simply accounts for the geometry of the expanding universe. The dynamics are on the right-hand side. Thus our goal is to compute the so-called "collision terms" that account for all processes changing the number of axions between the initial and final state and solve the resulting Boltzmann equation. After interactions stop happening, the right-hand side vanishes and the comoving axion number density $Y_a = n_a/s$ reaches a constant value Y_a^∞. The resulting contribution to the additional neutrino species results in $\Delta N_{\rm eff} \simeq 74.85\,(Y_a^\infty)^{4/3}$.

One can compute the production rate for each one of the operators in Eq. (2), and then calculate the number of axions produced if we switch on a single operator at the time [13–17]. However, this situation is not always realistic because once we write down a UV complete model multiple couplings contribute to axion production at different temperatures. Thus we need the production rate across the entire expansion history to quantify axion production for specific UV complete models.

The study in Ref. [18] completed the calculation for the axion production rate at all temperatures for the two most popular classes of axion models: KSVZ [9, 10] and DFSZ [11, 12]. For the former, none of the standard model particles transforms under PQ and the color anomaly is due to the presence of new heavy and colored fermions. For the latter, there are no new fermions in the spectrum and the color anomaly is due to standard model quarks.

A common feature of both frameworks, and actually of every UV complete model, is the presence of several mass thresholds across which the axion production rate changes its behavior drastically with the temperature. A threshold common to all PQ theories, which is a consequence of the interaction in Eq. (1) needed to solve the strong CP problem, is the QCD confinement scale. The analysis in Ref. [19] provided a continuous result for the production rate by extending previous calculations above such a scale, and with a smooth interpolation in the between. Another mass threshold present within the KSVZ framework is the one associated with the heavy-colored fermions responsible for the anomaly; the operator in Eq. (1) is local only well below their masses, and the fermions themselves are dynamical degrees of freedom mediating axion production at higher temperatures. For the DFSZ case the situation is ever richer due to the presence of several mass thresholds and the fact that all standard model particles are charged under PQ. First, this case features two Higgs doublets and the mass scale of the heavy Higgs bosons has to be taken into account carefully since axion interactions are super-renormalizable at high temperatures. Furthermore, the electroweak phase transition is another important cosmological phase across which the rate changes its behavior with the temperature significantly as discussed in detail by Ref. [16].

The production rate for the KSVZ axion across the expansion history is illustrated in Fig. 1. The mass of the heavy PQ-charge fermion is set to the value $m_\Psi = 10^5\,\mathrm{GeV}$ for illustration and consistently with collider bounds. We notice the different slope of the axion production rate above ($\gamma_a \propto T^4$) and below ($\gamma_a \propto T^6$) this mass threshold, and this is due to the fact that above axion production is mediated by a renormalizable interaction. The scaling for temperatures below m_Ψ persists until the confinement scale where it drops exponentially due to the Maxwell-Boltzmann suppression for the pion number density.

The analogous result for the DSFZ axion is illustrated in Fig. 2. The mass of the heavy Higgs boson is also set at around the same scale, $m_A \simeq 10^5\,\mathrm{GeV}$, and the detailed choice of the additional parameter $\tan\beta$ (the ratio of the vacuum expectation values of the two Higgs fields) does not affect the rate appreciably. As anticipated above, the structure is even richer here. Similarly to the previous case, axion production is mediated by a renormalizable operator at temperatures above m_A; the interaction is relevant in this case and therefore the rate scales as $\gamma_a \propto T^2$. Below the heavy Higgs bosons, dimension 5 coupling to standard model fermions (mostly top and bottom due to the larger Yukawa coupling) control the production rate that consequently scales as $\gamma_a \propto T^6$. Contrarily to the KSVZ case, fermion scatterings scaling as $\gamma_a \propto T^4$ dominate the production rate below the electroweak phase transition. Finally, pion scatterings are efficient as long as we do not hit the Maxwell-Boltzmann suppression. Nevertheless, axion production is active even well below the confinement scale since the axion couples to the muon and the electron.

We can insert these production rate into the Boltzmann equation in Eq. (6), and solve it to predict the amount of axion dark radiation expressed in terms of an effective number of additional neutrinos ΔN_{eff}. These predictions are shown in Figs. 3 and 4 for the KSVZ and DFSZ axion, respectively. The parameter chosen for the model are specified in the legend, and different lines correspond to different temperatures where the Boltzmann code begins its evolution with vanishing axion population in the early universe. We notice how the region probed currently by Planck is already excluded by supernovae bounds; it is worth keeping in mind that these astrophysical bounds come with their caveats, and it is beneficial to have a complementary probe of that parameter space region. Future CMB-S4 surveys have the potential of probing unexplored regions of the parameter space. This is particularly true for the KSVZ axion whereas the CMB-S4 discovery reach for the DFSZ axion is around the same region as the one for white dwarf bounds (present because the DFSZ axion couples to the electron).

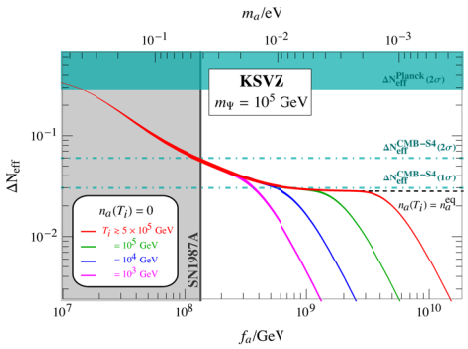

Figure 3. $\Delta N_{\rm eff}$ as a function of the axion decay constant for the KSVZ axion (from Ref. [18]).

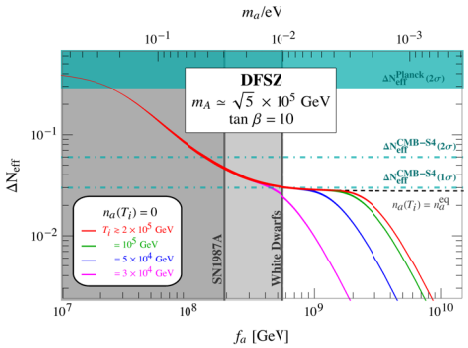

Figure 4. $\Delta N_{\rm eff}$ as a function of the axion decay constant for the DFSZ axion (from Ref. [18]).

3 Flavor-Violating Axion Couplings

A broad class of theories widely explored in the recent literature is the one where axion couplings to standard model fermions are non-diagonal. The general Lagrangian capturing all models where this happens reads

$$\mathcal{L}_{\rm FV}^{(a)} = \frac{\partial_\mu a}{2f_a} \sum_{\psi_i \neq \psi_j} \bar{\psi}_i \gamma^\mu \left(c^V_{\psi_i\psi_j} + c^A_{\psi_i\psi_j} \gamma^5 \right) \psi_j \,. \tag{7}$$

These flavor-violating couplings arise in theories connecting the origin of the SM flavor structure with the PQ symmetry. Even if the high-scale theory preserves the flavor symmetry, they can arise from quantum corrections due to flavor-violating standard model interactions. They are the target of several terrestrial experiments searching for rare meson decays. The early universe offers a complementary probe for this class of theories as well. The analysis by Ref. [20] performed a systematic study of these flavor-violating couplings by switching one operator at a time. For the first time, the contribution from binary scatterings was included and it was shown how it dominates completely the total axion production rate for the case of quarks. Scatterings were previously overlooked in the literature because decays always dominate unless there are hierarchies among the couplings mediating these processes. However, we can attach a QCD/QED interaction vertex to the three-point interactions in Eq. (7) and find a contribution proportional to the strong coupling constant. Furthermore, the treatment

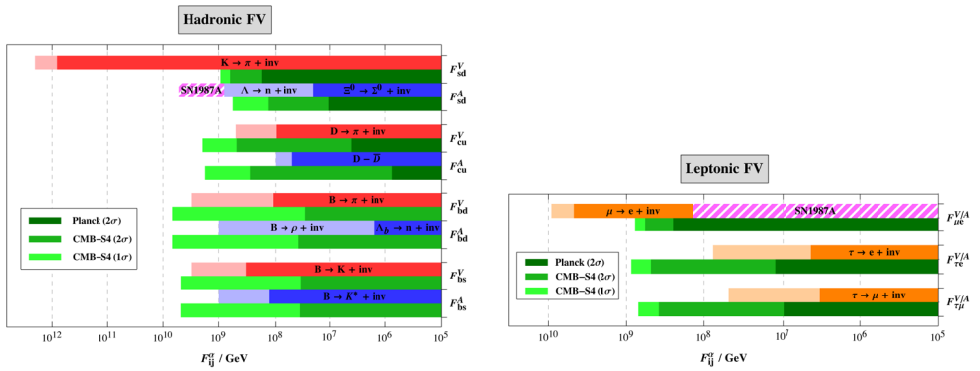

Figure 5. Current bounds and future prospects for flavor-violating axion interactions with quarks (left) and leptons (right). Figure from Ref. [20].

of the QCD crossover was improved via techniques analogous to the ones adopted for the flavor-conserving case.

The results in Fig. 5 show the comparison between terrestrial and cosmological bounds for flavor-violating axion interactions with quarks and leptons, respectively. Dark bands are current bounds, faint bands are projections for the future. The green bands (both dark and faint) show current and future cosmological bounds. For light quarks and leptons, we notice how laboratory searches perform better than cosmology. The situation changes once we include the third fermion generation where cosmology is competitive with terrestrial experiments and, in some cases, achieves better bounds.

4 Updated QCD Axion Mass Bounds

All the results presented so far neglected the axion mass. While this is definitely allowed at the time of BBN, it is not always the case at the time of recombination if the expression in Eq. (3) approaches values around 0.1 eV. The recent analysis by Ref. [21] incorporated a finite axion mass consistently, and the plots in Fig. 6 show the outcome of such a complete cosmological analysis that included also baryon acoustic oscillations (BAO) for the KSVZ and DFSZ axion, respectively.

We report the updated cosmological bounds on the axion mass

$$m_a \leq \begin{cases} 0.282\,(0.402)\ \text{eV} & \text{KSZV axion} \\ 0.209\,(0.293)\ \text{eV} & \text{DFSZ axion} \end{cases} . \tag{8}$$

Here, the results are shown at 95% and 99% CL, and the bound is stronger for the DFSZ axion because it couples to all standard model particles and more production channels contribute. These bounds, obtained with the production rates of Ref. [18], are about a factor of 5 stronger than the ones found by previous analysis that adopted approximate results for the rates.

5 What's next?

Thermal production of relativistic axions in the early universe is unavoidable if we have a thermal bath of standard model particles. This hot axion population leaves an imprint in the CMB for two broad classes of axion UV complete models. We point out also an intriguing

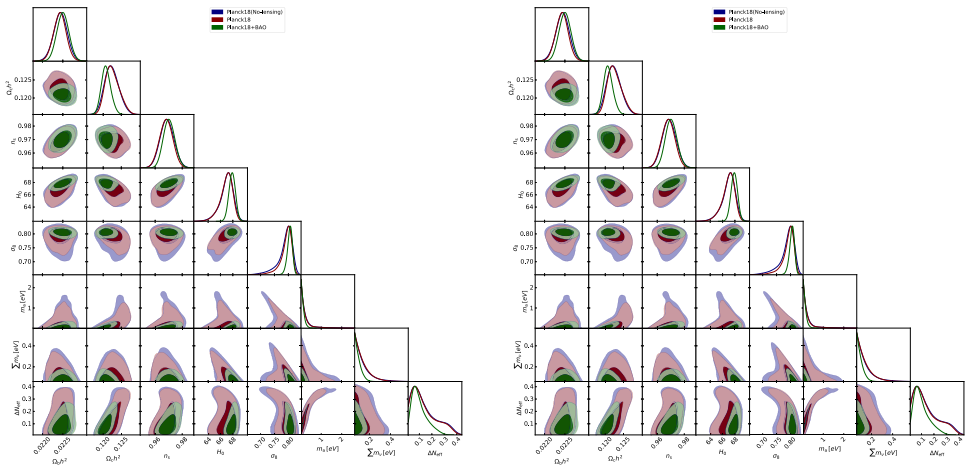

Figure 6. Allowed regions and one-dimensional probability posterior distributions for the KSVZ (left) and DFSZ (right) axion. Figure from Ref. [21].

interplay with flavor physics that we have just started to explore. The methodology presented here is general and it can be employed to analyze other microscopic models such as explicit scenarios of flavor-violating couplings.

There are still several directions in with we can improve our theoretical predictions. Broadly speaking, our goal is twofold: compute how many axions we produce, and connect this quantity with observables. Focusing on the first aspect, undoubtedly the one closer to the audience of this conference, the following questions are natural. How does production proceed above approximately 100 MeV? How do we describe the thermal bath in such a region? As it is conventional, we write down the expression for the rate as the combination of the number density of initial states and the thermal average of the cross section times the relative velocity. And there are improvements needed in both directions. Let us start with particle physics. Pion scattering needs to be improved at higher temperatures. And if we go to higher temperatures then we have other hadrons contributing too. Assuming we compute these cross sections reliably, we still need to know that to put for the number density. If the temperature is low enough (150 MeV) we can use the hadron resonance gas model, that is what is conventionally done, but what if we go to higher temperatures? Computing the cross sections is not enough. Last, but not least, there are many improvements needed also on the cosmological analysis part.

Given the solid motivation for the axion, and the large upcoming amount of cosmological data from CMB-S4 and large-scale structure surveys, it is important to provide reliable predictions to connect properly with data. The main source of uncertainty at the moment is due to QCD's strong dynamics.

Acknowledgements

This work was supported by: "The Dark Universe: A Synergic Multi-messenger Approach" number 2017X7X85K under the program PRIN 2017 funded by the Ministero dell'Istruzione, Università e della Ricerca (MIUR); "New Theoretical Tools for Axion Cosmology" under the Supporting TAlent in ReSearch@University of Padova (STARS@UNIPD). The author is supported by Istituto Nazionale di Fisica Nucleare (INFN) through the Theoretical Astroparticle

Physics (TAsP) project, and by the European Union's Horizon 2020 research and innovation programme under the Marie Skłodowska-Curie grant agreement No 860881-HIDDeN.

References

[1] R.D. Peccei, H.R. Quinn, Phys. Rev. Lett. **38**, 1440 (1977)
[2] R.D. Peccei, H.R. Quinn, Phys. Rev. D **16**, 1791 (1977)
[3] F. Wilczek, Phys. Rev. Lett. **40**, 279 (1978)
[4] S. Weinberg, Phys. Rev. Lett. **40**, 223 (1978)
[5] G. Grilli di Cortona, E. Hardy, J. Pardo Vega, G. Villadoro, JHEP **01**, 034 (2016), 1511.02867
[6] J. Preskill, M.B. Wise, F. Wilczek, Phys. Lett. B **120**, 127 (1983)
[7] L.F. Abbott, P. Sikivie, Phys. Lett. B **120**, 133 (1983)
[8] M. Dine, W. Fischler, Phys. Lett. B **120**, 137 (1983)
[9] J.E. Kim, Phys. Rev. Lett. **43**, 103 (1979)
[10] M.A. Shifman, A.I. Vainshtein, V.I. Zakharov, Nucl. Phys. B **166**, 493 (1980)
[11] A.R. Zhitnitsky, Sov. J. Nucl. Phys. **31**, 260 (1980)
[12] M. Dine, W. Fischler, M. Srednicki, Phys. Lett. B **104**, 199 (1981)
[13] R.Z. Ferreira, A. Notari, Phys. Rev. Lett. **120**, 191301 (2018), 1801.06090
[14] F. D'Eramo, R.Z. Ferreira, A. Notari, J.L. Bernal, JCAP **11**, 014 (2018), 1808.07430
[15] F. Arias-Aragón, F. D'Eramo, R.Z. Ferreira, L. Merlo, A. Notari, JCAP **11**, 025 (2020), 2007.06579
[16] F. Arias-Aragón, F. D'Eramo, R.Z. Ferreira, L. Merlo, A. Notari, JCAP **03**, 090 (2021), 2012.04736
[17] D. Green, Y. Guo, B. Wallisch, JCAP **02**, 019 (2022), 2109.12088
[18] F. D'Eramo, F. Hajkarim, S. Yun, JHEP **10**, 224 (2021), 2108.05371
[19] F. D'Eramo, F. Hajkarim, S. Yun, Phys. Rev. Lett. **128**, 152001 (2022), 2108.04259
[20] F. D'Eramo, S. Yun, Phys. Rev. D **105**, 075002 (2022), 2111.12108
[21] F. D'Eramo, E. Di Valentino, W. Giarè, F. Hajkarim, A. Melchiorri, O. Mena, F. Renzi, S. Yun, JCAP **09**, 022 (2022), 2205.07849